JACS
JOURNAL OF THE AMERICAN CHEMICAL SOCIETY

Communication

pubs.acs.org/JACS

Light-Fuelled Transport of Large Dendrimers and Proteins

Jenni E. Koskela,[†] Ville Liljeström,[†] Jongdoo Lim,[‡] Eric E. Simanek,[‡] Robin H.A. Ras,[†] Arri Priimagi,*[,†] and Mauri A. Kostiainen*[,§]

[†]Department of Applied Physics and [§]Department of Biotechnology and Chemical Technology, Aalto University, P.O. Box 15100, FI-00076 Aalto, Espoo, Finland

[‡]Department of Chemistry, Texas Christian University, Fort Worth, Texas 76129, United States

Supporting Information

ABSTRACT: This work presents a facile water-based supramolecular approach for light-induced surface patterning. The method is based upon azobenzene-functionalized high-molecular weight triazine dendrimers up to generation 9, demonstrating that even very large globular supramolecular complexes can be made to move in response to light. We also demonstrate light-fuelled macroscopic movements in native biomolecules, showing that complexes of apoferritin protein and azobenzene can effectively form light-induced surface patterns. Fundamentally, the results establish that thin films comprising both flexible and rigid globular particles of large diameter can be moved with light, whereas the presented material concepts offer new possibilities for the yet marginally explored biological applications of azobenzene surface patterning.

Azobenzenes are versatile photoswitches due to large, rapid, and reversible structural change upon cis−trans photoisomerization, which enables effective control over chemical, mechanical, and optical properties of azobenzene-containing systems.[1] The molecular-level isomerization can actuate motion on much larger length scale, even macroscopically.[2] As first discovered in 1995, illuminating a glassy azobenzene-containing polymer film with a light interference pattern results in the formation of temporally stable, high-modulation-depth surface-relief gratings (SRGs) on the polymer film.[3] Upon SRG formation polymer chains travel hundreds of nanometers across the substrate using light-fuelled azobenzene motors. The process is a complicated cascade of events depending on both the experimental parameters and the material itself. While researchers still debate the driving mechanism of mass transport,[4] the process is commonly acknowledged to originate from azobenzene photoisomerization. The versatility of azobenzene-based surface patterning renders it a useful tool, e.g., in photonic applications,[5] nanofabrication,[6] and for organizing other material systems such as liquid crystals and block copolymers.[7]

With their advantageous film-forming and mechanical properties, polymers offer a solid ground for studying structure-performance relations of SRG formation, both in covalent and supramolecular systems.[8] These studies have revealed, for instance, that the SRG formation process is highly sensitive to polymer molecular weight as chain entanglements can obstruct the macroscopic motions, even if some counter-examples exist.[9] Therefore, azobenzene-based molecular glasses have in recent years emerged as a new class of efficient SRG-forming materials.[10] Studying also other types of materials and the limits of azobenzene-based mass transport can shed new light on the surface patterning mechanism and lead to new, unprecedented uses of the surface patterns. One fundamental question yet to be answered is: what is the true size limit of molecules that can be transported with light-fuelled azobenzene motions?

Even if elementary materials-related studies on azobenzene SRG formation are of great importance, it is equally pertinent to consider their application potential and new fields where they could be utilized. As a photoswitch, azobenzene has been widely employed in functional biomaterials to be used in, e.g., light-controlled drug delivery, biomimetic nanochannels, and DNA hybridization.[11] However, only few reports have focused on the biological applications of azobenzene-based surface patterns.[12] While most nano/micropatterning methods rely on laborious laboratory protocols, azobenzene-containing materials enable fast and simple patterning of large surface areas with precise topography control at a length scale well-suited for, e.g., manipulating cell growth. In some cases the mass transport can be extremely efficient,[13] which may result in chemically heterogeneous surfaces that could be further functionalized for microarrays and sensing applications. Yet, to release the potential of azobenzene-based surface patterns in bioapplications, new biocompatible material concepts are still needed.

Dendrimers, highly branched globular macromolecules, are an advantageous choice for designing light-responsive materials. Dendritic molecules have a branched yet well-defined and monodisperse structure that can host functional groups both on the peripheral units[14] and in the core.[15] The light-responsive properties of azobenzene-functionalized dendritic structures have been studied for a variety of applications from light harvesting and optical anisotropy to film dewetting and drug release.[16] However, SRG-forming azo-dendrimers have so far received only limited attention.[17] Overall, the azo-dendrimer studies suggest that the structure and rigidity of the dendrimer dominate over size and generation in determining the optical response. This finding suggests that even very large dendrimers could exhibit attractive light-responsive properties when cleverly designed.

In this work, we show that surface patterns can be inscribed in thin films of high-molecular weight triazine dendrimers,

Received: March 14, 2014
Published: April 30, 2014

ACS Publications © 2014 American Chemical Society

synthesized and reported in 2013 by Lim et al.[18] and now functionalized with azobenzene via a facile supramolecular route. We also demonstrate that SRG inscription can be extended to native biomolecules, by utilizing azo-functionalized apoferritin protein films. To the best of our knowledge, light-induced surface patterns in a protein-based material have not been reported before. While the presented material concepts are of interest from a fundamental point-of-view for the study of azobenzene-based mass transport, they also hold promise for bioapplications of SRGs due to advantageous inherent properties of native biomolecules such as biocompatibility and ease of functionalization.

Triazine dendrimers of generations 3, 5, 7, and 9 were functionalized with a commercial azo dye, Ethyl Orange (EO). Complexation was carried out in dilute aqueous solution by the electrostatic attraction between the positively charged amine surface groups of the dendrimers and the negative sulfonic acid group of the chromophores. Complexation was confirmed by FTIR and UV–vis spectroscopy (see SI). A schematic structure of the generation 3 complex (G3-EO) is shown in Figure 1a

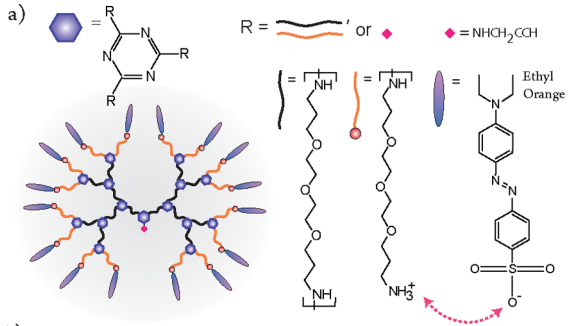

b)

	M_w of dendrimer	dendrimer diameter (nm)	number of end units	M_w of complex
G3-EO	7800	3.7	16	13 000
G5-EO	33 000	8.0	64	54 000
G7-EO	131 000	13.7	256	216 000
G9-EO	528 000	21.4	1024	868 000

Figure 1. (a) The chemical structure of the G3-EO complex and (b) the theoretical M_w and experimentally determined diameters of the dendrimers, the respective amount of end groups per dendrimer, and the M_w of nominally stoichiometric dendrimer–EO complexes.

(complete chemical structure in SI), with Figure 1b presenting the dendrimer sizes[18] and the weight-average molecular weights (M_w) of nominally stoichiometric complexes, containing ~40 weight % of EO. Water-based sample preparation is an important advantage for the use of the patterned surfaces in biological applications.

Dynamic light scattering (DLS) measurements were performed to characterize the supramolecular complex formation in dilute aqueous solution. Figure 2 shows the scattering intensity and particle mode size (the maximum of the size distribution) evolution as a function of EO/dendrimer ratio. Similar results were obtained for all generations (see SI). The DLS results indicate strong interaction between the azobenzene dyes and the dendrimers, as illustrated schematically in Figure 2 above the graph. Before adding EO, the dendrimers remain isolated in the solution. Above the stoichiometric EO amount of 0.5, the scattering intensity starts to increase strongly, indicating the formation of dense dendrimer–EO complexes, and peaks when

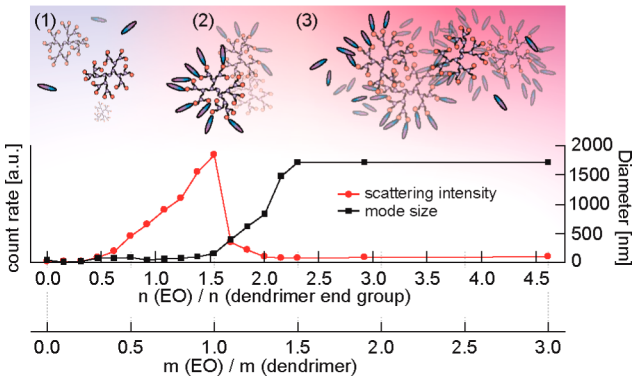

Figure 2. DLS scattering intensity and particle size evolution as a function of the EO/G7 ratio. At low EO concentrations the dendrimers remain isolated in the water solution (1), but increasing the amount of EO results in ionic complexation and aggregation of the complexes (2), which then swell at excess amount of EO (3).

the solution contains 1.5 EO molecules per dendrimer end group. At the same concentration, particle size increases rapidly, which we account for the formation of large swollen complex aggregates ($D_h \sim 1.7\ \mu m$), supported by the concurrent decrease in the scattering intensity. Atomic force microscopy (AFM) images of samples with varying stoichiometric amounts of EO (see SI) supported the DLS data.

For the surface patterning experiments, thin films with thicknesses ranging from 300 to 600 nm were prepared by spin coating the dendrimer–EO solutions on glass substrates. The samples were prepared from solutions with EO/dendrimer mass ratio of 1.5, and the thin films appeared homogeneous and of high optical quality. The UV–vis absorption spectra of the films (see the SI) are rather similar for all complexes, indicating that the local environment of the EO molecules is not very sensitive to dendrimer generation. Horizontally polarized laser light with wavelength of 488 nm and intensity of about 300 mW/cm^2 in a Lloyd's mirror setup was used for surface patterning (details in SI). Grating formation was monitored by recording diffraction from a nonisomerizing red laser beam, and the formed gratings were imaged with AFM.

Surface patterns were successfully inscribed in thin films of all complexes, irrespective of the dendrimer generation. An example diffraction curve is presented in Figure 3a for G5-EO. Importantly, gratings could only be inscribed with horizontally polarized light, while vertically polarized light yielded no diffraction. The polarization dependence is an unambiguous

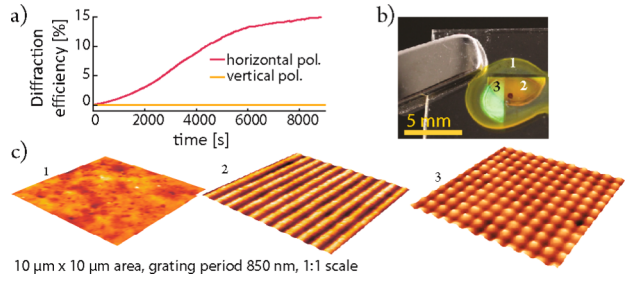

Figure 3. (a) Diffraction efficiency as a function of time for the G5-EO complex; (b) a photograph of a G5-EO sample film with two perpendicularly inscribed SRGs; and (c) the corresponding AFM images from (1) a flat (unilluminated) film, (2) a single grating, and (3) from the intersection of the two gratings.

dx.doi.org/10.1021/ja502623m | J. Am. Chem. Soc. 2014, 136, 6850–6853

proof that the SRG formation is driven by light, not by irreversible effects such as ablation or photodegradation, which are polarization independent. A photograph of a G5-EO film with two perpendicularly inscribed SRGs with corresponding AFM images of the gratings (10×10 μm) are presented in Figure 3b,c, respectively. Figure 4a shows the grating cross-section profiles

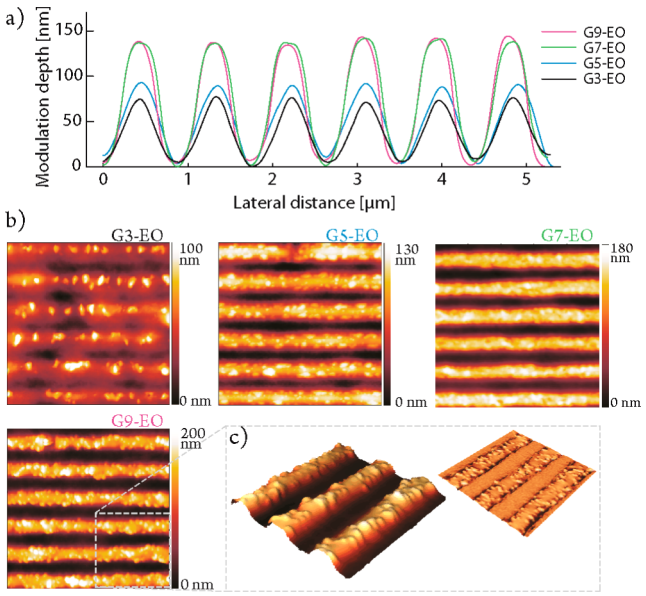

Figure 4. (a) SRG line profiles for all dendrimer–EO complexes; (b) AFM height images the SRGs (5×5 μm); and (c) 3D AFM height image (left) and phase image (right) of the G9-EO grating surface.

for all generations, while the AFM height images are shown in Figure 4b. Interestingly, the modulation depth of the SRGs increases with the dendrimer generation up to G7 and is equal for G7 and G9. This trend shows that the dendrimer size itself does not compromise the SRG inscription process but rather the opposite: larger dendrimer–EO complexes pile up as higher modulation-depth structures. These results indicate that increasing dendrimer generation poses no steric constraints on photoisomerization—a prerequisite for efficient SRG formation—as has also been observed by Archut et al.[17a] Also Gharagozloo et al. described comparable photo-orientation and SRG formation in star-branched polymers with different amount of branches but otherwise similar properties.[17b] Therefore, it seems that as long as the EO molecules form no microphase-separated domains,[17c] there is no apparent upper limit on dendrimer generation in the SRG formation process. To the best of our knowledge, light-induced movements in azo-dendrimers with generations exceeding 5 have not been studied previously.

The AFM images (Figure 4) also reveal rough surface textures on the SRGs of all complex generations, which likely originate from the complex aggregates present in the solution state (DLS results, Figure 2). It seems that the light-induced mass transport enhances the aggregation of the dendrimer–EO complexes, as the SRGs are rough only at the crests, whereas they appear as smooth at the troughs. This is further demonstrated in Figure 4c. Such aggregates are not found on the unilluminated areas of the sample films. This difference in surface roughness could be exploited, e.g., in applications in directed cell growth as cells can sense and react even to very small topographical differences.[19]

It is noteworthy that even the largest complex, G9-EO, is capable of forming SRGs in spite of its very large M_w of almost 900 kDa. We attribute this to the structure of the complex. The studied dendrimers are flexible, consisting of long hydrophilic chains connected with triazine rings. In contrast, EO is a rigid bulky molecule. When tightly bound to the dendrimer ionically, intermolecular interactions between EO molecules are not strong enough to form microphase-separated structure that may hinder mass transport.[17c] We believe that the dynamic nature of noncovalent bonding between the azo chromophores and the dendrimers plays an important role in the mass transport of the complexes. Bonding dynamics most likely also contributes to the aggregate formation on the fringes of the gratings.

To further push the limits of light-induced mass transport toward biological applications, we chose to study SRG formation in an azobenzene-containing protein material. In this case, the EO chromophores were mixed with ferritin, a ubiquitous intracellular iron-storage protein, which is a hollow globular shell (apoferritin, aFT) with diameter of 12 nm and M_w of 450 kDa. Ferritins and other protein cages are an interesting class of nanoparticles due to their well-defined hollow structure and ability to encapsulate various synthetic and biological materials.[20] The M_w of aFT falls into the range between G7 and G9 dendrimers, but its structure and rigidity are significantly different. aFT behaves as a rigid sphere consisting of tightly arranged protein subunits, while the dendrimers have more freedom in terms of shape. On the other hand, binding between EO and the protein is not as well-defined as with the dendrimers.

In order to electrostatically bind the negatively charged EO to aFT, we measured DLS from aFT solution where pH < pI and the protein carries a net positive charge. The results are shown in Figure 5a,b, indicating that when EO is added, the scattering

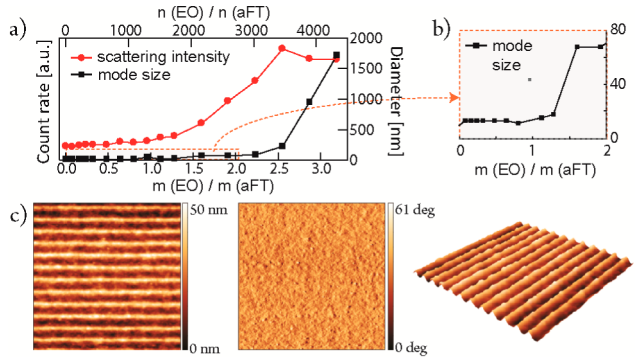

Figure 5. (a) DLS data from aFT-EO in aqueous solution. Scattering intensity and particle size evolution as a function of the EO/aFT ratio, with b) a zoom-in of the 0–80 nm range of particle mode size. (c) a 10×10 μm AFM height image of an SRG on the aFT-EO film, with the corresponding phase image and a 3D presentation.

intensity increases slowly until the mass ratio of 1.5, after which it rises much more rapidly, while the average particle size increases from 12 to ~70 nm. We interpret this as the formation of protein–azo complexes. With an excess amount of EO, at mass ratio of 2.5, also the average size grows rapidly while intensity levels off, indicating that the complexes start to aggregate.

Thin films of aFT-EO were prepared by spin-coating from aqueous solution with EO/aFT mass ratio of 1. Small-angle X-ray scattering measurument (SI) proved the films to be amorphous. Surface patterning was performed in the same way as with the dendrimer–EO samples, with the exception that the illumination was stopped at 40 min after the diffraction efficiency had leveled off (note that for the dendrimer–EO complexes it takes >2 h for

dx.doi.org/10.1021/ja502623m | J. Am. Chem. Soc. 2014, 136, 6850–6853

the SRG inscription process to saturate). AFM confirmed the formation of an SRG with an average modulation depth of approximately 50 nm, as presented in Figure 5c. Unlike in the dendrimer−EO films, the SRG inscribed in aFT-EO does not show up in the AFM phase image, and the material appears similar throughout the grating area. Judging by the faster saturation of diffraction efficiency, the smaller modulation depth, and the different surface texture, the dynamics of SRG formation differ quite drastically between the protein and the dendrimer complexes due to their structural differences. Importantly, these results demonstrate that a solid film comprising large and rigid spherical particles can be structured with azobenzene and light. The azo-based topographical patterning could be combined with the intrinsic capability of aFT to host other material inside the protein cage, e.g., to produce surfaces for guided cell growth with both chemical and physical cues.

In conclusion, we have shown that very large complexes of triazine dendrimers and azobenzene chromophores are able to undergo mass transport and form topographical surface patterns under illumination. This result establishes the feasibility of high-generation dendritic structures as host material in photo-responsive systems, highlighting that the globular molecular architecture enables even very large molecules to move in response to light. Furthermore, the concept has been applied, for the first time, to induce surface patterns in a film of an azobenzene-functionalized native protein. Essentially, the results extend the limits of azobenzene-induced surface patterning, showing that thin films of both flexible and hard spheres with relatively large diameter can be moved with light. The results are important from both fundamental and applied perspectives, where the use of unconventional material choices provides new insights in the surface patterning phenomenon itself. Also, we envision a realm of new opportunities for creating patterned surfaces of other type of azo-functionalized native biomolecules and spherical particles such as synthetic metal nanoparticles.

■ ASSOCIATED CONTENT

Supporting Information

Experimental details and characterization data. This material is available free of charge via the Internet at http://pubs.acs.org.

■ AUTHOR INFORMATION

Corresponding Author

arri.priimagi@aalto.fi; mauri.kostiainen@aalto.fi

Notes

The authors declare no competing financial interest.

■ ACKNOWLEDGMENTS

Academy of Finland (projects 135159, 267497, 273645, and 263504), Welch Foundation (A-0008), and Emil Aaltonen Foundation (project 700023) are acknowledged for financial support. This work made use of The Aalto University Nanomicroscopy Center (Aalto-NMC) premises.

■ REFERENCES

(1) (a) Natansohn, A.; Rochon, P. *Chem. Rev.* **2002**, *102*, 4139. (b) Russew, M.-M.; Hecht, S. *Adv. Mater.* **2010**, *22*, 3348.

(2) (a) Yu, H.; Ikeda, T. *Adv. Mater.* **2011**, *23*, 2149. (b) Iamsaard, S.; Aßhoff, S. J.; Matt, B.; Kudernac, T.; Cornelissen, J. J. L. M.; Fletcher, S. P.; Katsonis, N. *Nat. Chem.* **2014**, *6*, 229. (c) Mahimwalla, Z.; Yager, K. G.; Mamiya, J.; Shishido, A.; Priimagi, A.; Barrett, C. J. *Polym. Bull.* **2012**, *69*, 967.

(3) (a) Rochon, P.; Batalla, E.; Natansohn, A. *Appl. Phys. Lett.* **1995**, *66*, 136. (b) Kim, D. Y.; Tripathy, S. K.; Li, L.; Kumar, J. *Appl. Phys. Lett.* **1995**, *66*, 1166.

(4) (a) Juan, M. L.; Plain, J.; Bachelot, R.; Royer, P.; Gray, S. K.; Wiederrecht, G. P. *ACS Nano* **2009**, *3*, 1573. (b) Ambrosio, A.; Maddalena, P.; Marrucci, L. *Phys. Rev. Lett.* **2013**, *110*, 146102.

(5) (a) Ishow, E.; Brosseau, A.; Clavier, G.; Nakatani, K.; Pansu, R. B.; Vachon, J.-J.; Tauc, P.; Chauvat, D.; Mendonça, C. R.; Piovesan, E. *J. Am. Chem. Soc.* **2007**, *129*, 8970. (b) Goldenberg, L. M.; Lisinetskii, V.; Schrader, S. *Adv. Opt. Mater.* **2013**, *1*, 527. (c) Kang, J.-W.; Kim, M.-J.; Kim, J.-P.; Yoo, S.-J.; Lee, J.-S.; Kim, D. Y.; Kim, J.-J. *Appl. Phys. Lett.* **2003**, *82*, 3823. (d) Priimagi, A.; Shevchenko, A. *J. Polym. Sci., Part B: Polym. Phys.* **2014**, *52*, 163.

(6) (a) Lee, S.; Kang, H. S.; Park, J.-K. *Adv. Mater.* **2012**, *24*, 2069. (b) Moerland, R. J.; Koskela, J. E.; Kravchenko, A.; Simberg, M.; van der Vegte, S.; Kaivola, M.; Priimagi, A.; Ras, R. H. A. *Mater. Horiz.* **2014**, *1*, 74.

(7) (a) Shteyner, E. A.; Srivastava, A. K.; Chigrinov, V. G.; Kwok, H.-S.; Afanasyev, A. D. *Soft Matter* **2013**, *9*, 5160. (b) Snell, K. E.; Stéphant, N.; Pansu, R. B.; Audibert, J.-F.; Lagugné-Labarthet, F.; Ishow, E. *Langmuir* **2014**, *30*, 2926. (c) Morikawa, Y.; Nagano, S.; Watanabe, K.; Kamata, K.; Iyoda, T.; Seki, T. *Adv. Mater.* **2006**, *18*, 883.

(8) Seki, T. *Macromol. Rapid Commun.* **2014**, *35*, 271.

(9) Yang, S.; Li, L.; Cholli, A. L.; Kumar, J.; Tripathy1†, S. K. *J. Macromol. Sci., Part A: Pure Appl. Chem.* **2001**, *38*, 1345.

(10) (a) Nakano, H.; Takahashi, T.; Kadota, T.; Shirota, Y. *Adv. Mater.* **2002**, *14*, 1157. (b) He, Y.; Gu, X.; Guo, M.; Wang, X. *Opt. Mater.* **2008**, *31*, 18. (b) Goldenberg, L. M.; Kulikovsky, L.; Kulikovska, O.; Tomczyk, J.; Stumpe, J. *Langmuir* **2010**, *26*, 2214.

(11) (a) Beharry, A. A.; Woolley, G. A. *Chem. Soc. Rev.* **2011**, *40*, 4422. (b) Zhang, J.; Wang, J.; Tian, H. *Mater. Horiz.* **2014**, *1*, 169.

(12) (a) Baac, H.; Lee, J.-H.; Seo, J.-M.; Park, T. H.; Chung, H.; Lee, S.-D.; Kim, S. J. *Mater. Sci. Eng., C* **2004**, *24*, 209. (b) Hurduc, N.; Macovei, A.; Paius, C.; Raicu, A.; Moleavin, I.; Branza-Nichita, N.; Hamel, M.; Rocha, L. *Mater. Sci. Eng., C* **2013**, *33*, 2440. (c) Barillé, R.; Janik, R.; Kucharski, S.; Eyer, J.; Letournel, F. *Colloids Surf., B* **2011**, *88*, 63.

(13) Priimagi, A.; Saccone, M.; Cavallo, G.; Shishido, A.; Pilati, T.; Metrangolo, P.; Resnati, G. *Adv. Mater.* **2012**, *24*, OP345.

(14) Puntoriero, F.; Ceroni, P.; Balzani, V.; Bergamini, G.; Vögtle, F. *J. Am. Chem. Soc.* **2007**, *129*, 10714.

(15) Jiang, D.; Aida, T. *Nature* **1997**, *388*, 454.

(16) (a) Marchi, E.; Baroncini, M.; Bergamini, G.; Van Heyst, J.; Vögtle, F.; Ceroni, P. *J. Am. Chem. Soc.* **2012**, *134*, 15277. (b) Deloncle, R.; Caminade, A.-M. *J. Photochem. Photobiol., C* **2010**, *11*, 25. (c) Hernández-Ainsa, S.; Alcalá, R.; Barberá, J.; Marcos, M.; Sánchez, C.; Serrano, J. L. *Macromolecules* **2010**, *43*, 2660. (d) Del Barrio, J.; Blasco, E.; Toprakcioglu, C.; Koutsioubas, A.; Scherman, O. A.; Oriol, L.; Sánchez-Somolinos, C. *Macromolecules* **2014**, *47*, 897.

(17) (a) Archut, A.; Vögtle, F.; De Cola, L.; Azzellini, G. C.; Balzani, V.; Ramanujam, P. S.; Berg, R. H. *Chem.—Eur. J.* **1998**, *4*, 699. (b) Gharagozloo-Hubmann, K.; Kulikovska, O.; Börger, V.; Menzel, H.; Stumpe, J. *Macromol. Chem. Phys.* **2009**, *210*, 1809. (c) Vapaavuori, J.; Priimagi, A.; Soininen, A. J.; Canilho, N.; Kasëmi, E.; Ruokolainen, J.; Kaivola, M.; Ikkala, O. *Opt. Mater. Express* **2013**, *3*, 711. (d) Li, W.; Dohi, T.; Hara, M.; Nagano, S.; Haba, O.; Yonetake, K.; Seki, T. *Macromolecules* **2012**, *45*, 6618.

(18) Lim, J.; Kostiainen, M.; Maly, J.; da Costa, V. C. P.; Annunziata, O.; Pavan, G. M.; Simanek, E. E. *J. Am. Chem. Soc.* **2013**, *135*, 4660.

(19) Ross, A. M.; Lahann, J. *J. Polym. Sci., Part B: Polym. Phys.* **2013**, *51*, 775.

(20) (a) Uchida, M.; Klem, M. T.; Allen, M.; Suci, P.; Flenniken, M.; Gillitzer, E.; Varpness, Z.; Liepold, L. O.; Young, M.; Douglas, T. *Adv. Mater.* **2007**, *19*, 1025. (b) Kostiainen, M. A.; Ceci, P.; Fornara, M.; Hiekkataipale, P.; Kasyutich, O.; Nolte, R. J. M.; Cornelissen, J. J. L. M.; Desautels, R. D.; van Lierop, J. *ACS Nano* **2011**, *5*, 6394. (c) Kostiainen, M. A.; Hiekkataipale, P.; Laiho, A.; Lemieux, V.; Seitsonen, J.; Ruokolainen, J.; Ceci, P. *Nat. Nanotechnol.* **2013**, *8*, 52.